Intracellular calcium clearance in Purkinje cell somata from rat cerebellar slices

Leonardo Fierro, Reinaldo DiPolo* and Isabel Llano

*Arbeitsgruppe Zelluläre Neurobiologie, Max-Planck-Institut für Biophysikalische Chemie, Am Fassberg, D37070 Göttingen, Germany and *Laboratorio de Permeabilidad Iónica, Centro de Biofísica y Bioquímica, Instituto Venezolano de Investigaciones Científicas, Caracas-1020A, Venezuela*

(Received 17 December 1997; accepted after revision 7 April 1998)

1. The mechanisms governing the return of intracellular calcium (Ca_i^{2+}) to baseline levels following depolarization-evoked $[Ca^{2+}]_i$ rises were investigated in Purkinje cell somata using tight-seal whole-cell recordings and fura-2 microfluorometry, for peak $[Ca^{2+}]_i$ ranging from 50 nM to 2 μM.

2. Ca_i^{2+} decay was well fitted by a double exponential with time constants of 0·6 and 3 s. Both time constants were independent of peak $[Ca^{2+}]_i$ but the contribution of the faster component increased with $[Ca^{2+}]_i$.

3. Thapsigargin (10 μM) and cyclopiazonic acid (50 μM) prolonged Ca_i^{2+} decay indicating that sarco-endoplasmic reticulum Ca^{2+} (SERCA) pumps contribute to Purkinje cell Ca_i^{2+} clearance.

4. A modest participation in clearance was found for the plasma membrane Ca^{2+} (PMCA) pumps using 5,6-succinimidyl carboxyeosin (40 μM).

5. The Na^+–Ca^{2+} exchanger also contributed to the clearance process, since replacement of extracellular Na^+ by Li^+ slowed Ca_i^{2+} decay.

6. Carbonyl cyanide *m*-chlorophenylhydrazone (CCCP, 2 μM) and rotenone (10 μM) increased $[Ca^{2+}]_i$ and elicited large inward currents at −60 mV. Both effects were also obtained with CCCP in the absence of external Ca^{2+}, suggesting that mitochondrial Ca^{2+} uptake uncouplers release Ca^{2+} from intracellular stores and may alter the membrane permeability to Ca^{2+}. These effects were irreversible and impeded tests on the role of mitochondria in Ca_i^{2+} clearance.

7. The relative contribution of the clearance systems characterized in this study varied as a function of $[Ca^{2+}]_i$. At 0·5 μM Ca_i^{2+}, SERCA pumps, PMCA pumps and the Na^+–Ca^{2+} exchanger contribute equally to removal and account for 78% of the process. Only 45% of the removal at 2 μM Ca_i^{2+} can be explained by these systems. In this high $[Ca^{2+}]_i$ range the major contribution is that of SERCA pumps (21%) and of the Na^+–Ca^{2+} exchanger (18%), whereas the contribution of PMCA pumps is only 6%.

Variations in intracellular calcium (Ca_i^{2+}) levels play crucial roles in information processing in cerebellar Purkinje cells, since several forms of synaptic plasticity at their excitatory (Sakurai, 1990) and inhibitory inputs (reviewed by Marty & Llano, 1995) are triggered by $[Ca^{2+}]_i$ rises. Transient changes in dendritic $[Ca^{2+}]_i$ can be elicited by stimulation of the two excitatory synaptic inputs converging on Purkinje cells: climbing and parallel fibres (Miyakawa, Lev-Ram, Lasser-Ross & Ross, 1992; Denk, Sugimori & Llinás, 1995). Activation of voltage-gated Ca^{2+} channels leads to large increases in dendritic (Tank, Sugimori, Connor & Llinás, 1988; Lev-Ram, Miyakawa, Lasser-Ross & Ross, 1992) as well as in somatic $[Ca^{2+}]_i$ (Kano, Schneggenburger, Verkhratsky & Konnerth, 1995), and these signals can be amplified by calcium-induced calcium release (CICR; Llano, DiPolo & Marty, 1994). Confocal imaging has shown that climbing fibre activation produces substantial increases in $[Ca^{2+}]_i$, not only in Purkinje cell dendrites, but also in the cell somata (Eilers, Callewaert, Armstrong & Konnerth, 1995).

Cerebellar Purkinje cells have powerful systems to control $[Ca^{2+}]_i$. Immunocytochemical studies demonstrate considerable amounts of Ca^{2+}-binding proteins, particularly calbindin D_{28k} and parvalbumin (Tolosa de Talamoni, Smith, Wasserman, Beltramino, Fullmer & Penniston, 1993). Calsequestrin, a well-known constituent of skeletal muscle sarcoplasmic reticulum which is not found in other

neurones, has also been reported (Takei *et al.* 1992, and references therein). Concerning potential sources of Ca^{2+} release from intracellular stores (reviewed by Ogden, 1996), Purkinje cells express different forms of inositol trisphosphate receptors (InsP_3Rs), as well as of ryanodine receptors (RyRs); they are unique among CNS neurones in expressing the skeletal type of RyRs. Rises in $[Ca^{2+}]_i$ mediated by activation of InsP_3Rs (Khodakhah & Ogden, 1995, and references therein) and RyRs (Llano *et al.* 1994) have been demonstrated in Purkinje cells.

In addition to these unusual characteristics, other ubiquitous systems involved in Ca_i^{2+} homeostasis have been described in Purkinje cells. By immunocytochemical techniques the presence of sarco-endoplasmic reticulum Ca^{2+} (SERCA) pumps has been recognized (Plessers, Eggermont, Wuytack & Casteels, 1991). SERCA pumps are particularly abundant at the level of the endoplasmic reticulum cisterns (Takei *et al.* 1992, and references therein). The plasma membrane Ca^{2+} (PMCA) pumps are ubiquitous in the plasma membrane of Purkinje cells (Tolosa de Talamoni *et al.* 1993).

Although several studies on dendritic Ca_i^{2+} dynamics in Purkinje cells have been performed (reviewed in Regehr & Tank, 1994), little is known of the kinetics of Ca_i^{2+} removal at the somata and dendrites of these neurones. In a previous paper we showed that Purkinje cells have a very high Ca^{2+}-binding ratio which endows them with the ability to efficiently handle large Ca_i^{2+} loads (Fierro & Llano, 1996). Because buffers confiscate Ca^{2+}, they decrease the effective extrusion rates of clearance mechanisms which are only effective on freely diffusing Ca^{2+} ions. Therefore, the presence of very strong buffers suggests that Purkinje cells extrude Ca^{2+} at slow rates, or else, that they should have particularly efficient clearance systems. In the present work, we study the mechanisms responsible for Ca_i^{2+} clearance at Purkinje cell somata and describe their respective contributions to the removal process in the range of $[Ca^{2+}]_i$ increments pertaining to physiological activity.

METHODS

The procedures for preparation of cerebellar slices and subsequent tight-seal whole-cell recordings (WCR) combined with fluorometric fura-2 measurements have been described in detail in a recent publication (Fierro & Llano, 1996). In the present study, cerebellar slices were obtained from 12- to 17-day-old rats, decapitated following cervical dislocation. The external saline had a composition of (mM): 125 NaCl, 2·5 KCl, 2 $CaCl_2$, 1 $MgCl_2$, 1·25 NaH_2PO_4, 26 $NaHCO_3$ and 10 glucose (pH of 7·4 when equilibrated with a mixture of 95% O_2 and 5% CO_2; 295–300 mosmol l^{-1}). The experimental chamber was perfused at a rate of 0·8–1 ml min^{-1} with this saline, complemented with tetrodotoxin (200 nM) and the $GABA_A$ receptor antagonist bicuculline methochloride (10 μM). WCR was performed with pipettes filled with a solution containing (mM): 150 CsCl, 4·6 $MgCl_2$, 10 Hepes acid, 0·4 Na-GTP and 4 Na_2-ATP (pH adjusted to 7·34 with *N*-methyl-D-glucamine; 295–300 mosmol l^{-1}). Unless otherwise noted, 250 μM fura-2 was included in the pipette solution. Experiments were done at room temperature (20–24 °C).

All reagents were purchased from Sigma, except bicuculline methochloride (Tocris Neuramin), thapsigargin (Calbiochem), 5,6-succinimidyl carboxyeosin (Molecular Probes) and fura-2 (Molecular Probes). Thapsigargin, carbonyl cyanide *p*-trifluoromethoxyphenylhydrazone (FCCP), carbonyl cyanide *m*-chlorophenylhydrazone (CCCP), oligomycin, rotenone, 5,6-succinimidyl carboxyeosin and cyclopiazonic acid were dissolved in DMSO and stored at −20 °C. Final concentrations of DMSO never exceeded 0·01%, a concentration which does not affect Ca_i^{2+} levels.

Experimental protocols and analysis routines

Most of the experiments in this work involve comparisons of the rate of decay of pulse-evoked $[Ca^{2+}]_i$ rises in control external saline and after the application of an inhibitor of a putative Ca_i^{2+} clearance system. Cells were held at −60 mV and Ca_i^{2+} transients were elicited by depolarizing pulses of 20–300 ms duration to 0 mV. The membrane current and the fluorescence signal resulting from 390 nm excitation were acquired at a sampling rate of 1 ms $point^{-1}$ during the 10 s following the voltage step. Average values of the fluorescence at the isosbestic point (F_{360}) were obtained from 100 ms exposures to 360 nm light immediately before and after the 390 nm excitation. These values were interpolated to generate a data set of F_{360} *versus* time, containing the same number of points as the 390 nm data. The two data sets were then divided point by point, and from the resulting ratio values (F_{360}/F_{390}) $[Ca^{2+}]_i$ was calculated as explained in Fierro & Llano (1996). To examine the contribution of the different mechanisms to the decay of Ca_i^{2+} transients, a series of pulses of different duration was applied at 90 s intervals in control saline. Four to five minutes after adding the inhibitor the series of pulses was repeated. This protocol was used in all the experiments, unless otherwise stated in the figure legends.

To estimate the contribution of each system to the return of $[Ca^{2+}]_i$ to baseline levels, Ca_i^{2+} transients which reached similar peak values in control and test conditions were chosen and the clearance rate was calculated as follows. (i) The decay phase of each transient was fitted by a single or a double exponential function and the derivative function ($d[Ca^{2+}]_i/dt$) was calculated from the fit. (ii) $-d[Ca^{2+}]_i/dt$ was then plotted as a function of the $[Ca^{2+}]_i$ values obtained from the exponential fit. (iii) The plots from transients with equal peak $[Ca^{2+}]_i$ in each condition (control *versus* inhibitor) were pooled and fitted with a polynomial function of fifth to seventh order. (iv) The polynomial fit calculated for the inhibitor condition was subtracted from the polynomial fit calculated from the control data, to yield the mean contribution to Ca_i^{2+} clearance of the system studied as a function of $[Ca^{2+}]_i$.

To explore the effects of experimental manipulations on the resting calcium concentration, $[Ca^{2+}]_R$, the fluorescence resulting from 200 ms paired exposures to 360 and 390 nm light was acquired and used to calculate $[Ca^{2+}]_R$. When the external solution was replaced by a Ca^{2+}-free saline (no added Ca^{2+} plus 200 μM EGTA; e.g. Fig. 6*C*), depolarizing pulses from −60 to 0 mV were applied before and after Ca^{2+} removal to assess the effectiveness of the solution exchange. In general, 8 min after the slice was perfused with Ca^{2+}-free saline, complete Ca^{2+} removal from the extracellular media was reached as evidenced by the lack of $[Ca^{2+}]_i$ rises upon depolarization.

RESULTS

Decay of Ca_i^{2+} transients in Purkinje cell somata

In this section, we describe the general properties of the return of $[Ca^{2+}]_i$ to baseline levels following depolarization-induced $[Ca^{2+}]_i$ rises in Purkinje cell somata. In these

experiments, resting $[Ca^{2+}]_i$ was 25 ± 10 nM ($n = 20$; mean ± S.D.) and depolarizing pulses of increasing duration (50–300 ms) induced transient rises in $[Ca^{2+}]_i$ to peak levels ranging from 50 nM to 2 μM. The rising phase of the pulse-evoked transients showed a biphasic behaviour in the high $[Ca^{2+}]_i$ range, indicative of CICR (Llano *et al.* 1994). As shown in Fig. 1*A*, throughout most of the $[Ca^{2+}]_i$ range explored, the return of $[Ca^{2+}]_i$ to baseline levels was well described by a double exponential function with a fast time constant (τ_1) of the order of 700 ms and a slow time constant (τ_2) of the order of 4 s (fits are superimposed on the traces). Biexponential decays were observed in all cells analysed ($n = 110$) for peak Ca_i^{2+} levels over 300 nM. At lower peak Ca_i^{2+} levels, 50% of the cells had transients which were well approximated by a single exponential function. In these cases, the apparent threshold between a monophasic and a biphasic decay ranged from 100 to 280 nM. Figures 1*B* and *C* present the pooled data from ten of the cells exhibiting biexponential decay throughout the $[Ca^{2+}]_i$ range studied. The plots of τ_1 and τ_2 as a function of the peak value of $[Ca^{2+}]_i$ (Fig. 1*B*) indicate little dependence of both time constants on peak $[Ca^{2+}]_i$. However, the contribution of each component to the biphasic decay varies as function of peak $[Ca^{2+}]_i$: the fast component dominates above 0·5 μM Ca_i^{2+} whereas the slow component dominates at lower peak $[Ca^{2+}]_i$ (Fig. 1*C*). This behaviour translates to a decrease in the time required for $[Ca^{2+}]_i$ to decay to 50% of its peak value as the peak $[Ca^{2+}]_i$ increases (see Fig. 2*B*).

Two sets of experiments were carried out to ascertain that the time course of the decay of Ca_i^{2+} transients was not affected by the experimental procedures used in the present work. Firstly, we verified that the use of fura-2 at 250 μM did not slow-down Ca_i^{2+} transients. The addition of a high-affinity Ca^{2+} buffer, such as fura-2, can alter the kinetics of Ca_i^{2+} signals (Sala & Hernández-Cruz, 1990) to an extent set by the properties of the endogenous buffers (reviewed by Neher, 1995). Purkinje cells have an unusually high Ca^{2+}-binding ratio (Fierro & Llano, 1996) and thus addition of 250 μM fura-2 should not interfere with the endogenous systems. To verify this point, the time course of the decay

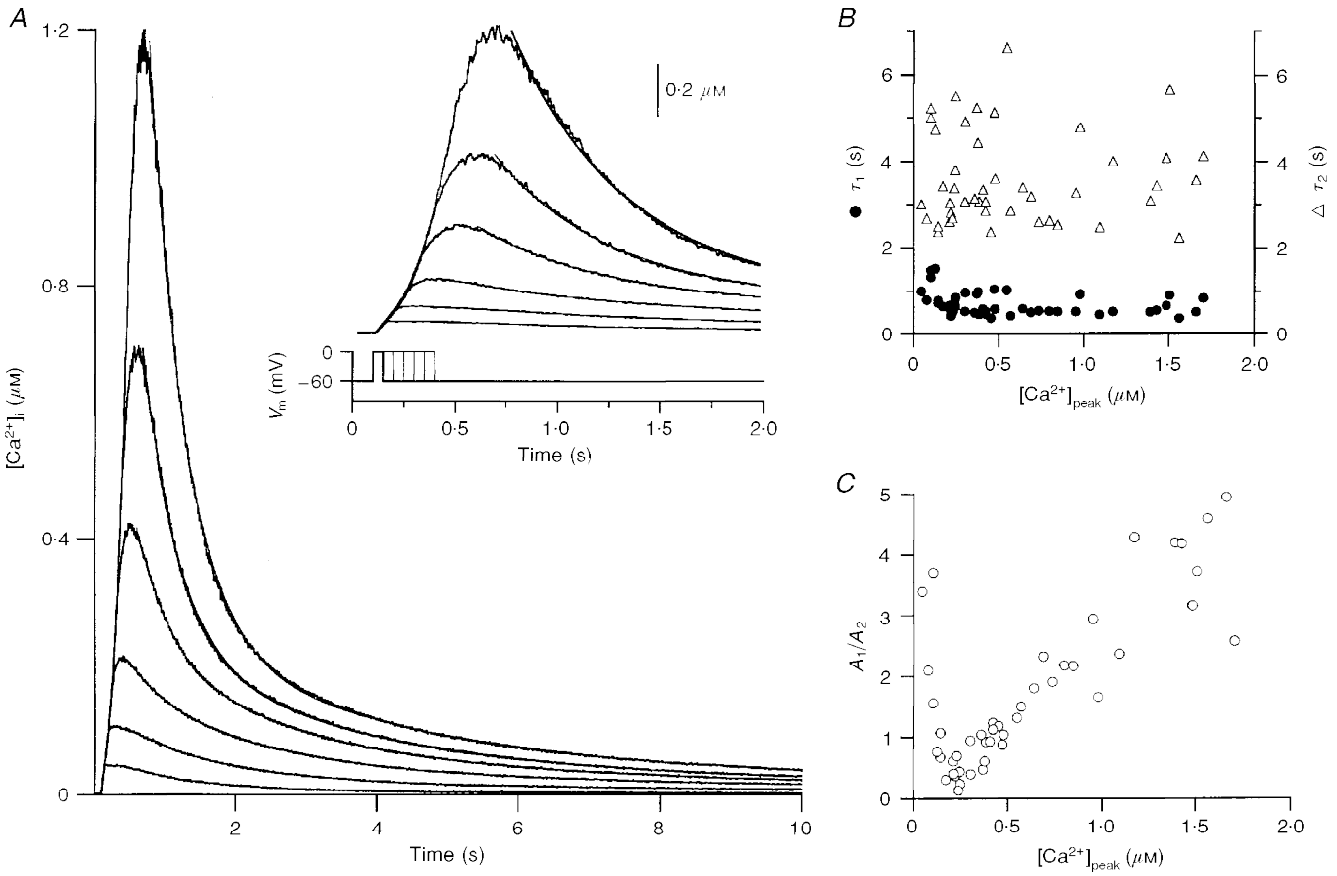

Figure 1. Decay of Ca_i^{2+} transients in cerebellar Purkinje cell somata

A, representative Ca_i^{2+} transients elicited by depolarizations of durations ranging from 50 to 300 ms (steps of 50 ms, as shown in lower part of inset). Double exponential fits of the decay phase are superimposed on each trace. An expanded view of the same data is displayed in the inset. In this and subsequent figures, the holding potential was set to −60 mV and the pulse brought the membrane potential to 0 mV. *B*, pooled data (10 cells) for the value of the time constants of the decay of Ca_i^{2+} transients (τ_1 and τ_2) as a function of peak $[Ca^{2+}]_i$ ($[Ca^{2+}]_{peak}$). *C*, plot of the ratio of the corresponding amplitude coefficients (A_1/A_2) as a function of peak $[Ca^{2+}]_i$ for the same cells as in *B*.

of pulse-evoked Ca_i^{2+} transients was compared in cells dialysed with 25 ($n = 11$) and 250 μM fura-2 ($n = 14$), as shown in Fig. 2*A*. To quantify these experiments, each transient was analysed in terms of $t_{0.5}$ (the time at which $[Ca^{2+}]_i$ decayed to 50% of its peak), and the data, binned at 100 nM increments in peak $[Ca^{2+}]_i$, were plotted as a function of peak $[Ca^{2+}]_i$. The results, displayed in Fig. 2*B*, confirm that Ca_i^{2+} decay is not affected by fura-2 concentration in the 25–250 μM range.

We next determined the behaviour of Ca_i^{2+} decay as a function of WCR time, to rule out possible effects of washout of cytoplasmic components on Ca_i^{2+} homeostasis. Ca_i^{2+} transients were elicited by depolarizing steps repeated at 2 min intervals, starting 4 min after breaking into the cell and followed for the ensuing 32–34 min. Figure 2*C* presents superimposed Ca_i^{2+} transients obtained from two different cells at the indicated times in WCR, for stimuli raising $[Ca^{2+}]_i$ to ~300 nM (upper panel) and ~1 μM (lower panel). The time course of decay of the signals is quite similar, irrespective of the time in WCR. The pooled data ($n = 10$) for $t_{0.5}$ as a function of WCR time displayed in Fig. 2*D* demonstrate that the decay phase of Ca_i^{2+} transients is stable within a time window ranging from 6 to 30 min after establishment of the WCR configuration. Therefore, the experiments described in the remaining sections were collected from 8 to 28 min after breaking into the cell.

Mechanisms contributing to Ca_i^{2+} clearance in Purkinje cell somata

In most cell types studied, two main types of mechanism regulate the time course of decay of Ca_i^{2+} transients: those which sequester Ca^{2+} ions into intracellular stores and those which transport the ions towards the extracellular space. In

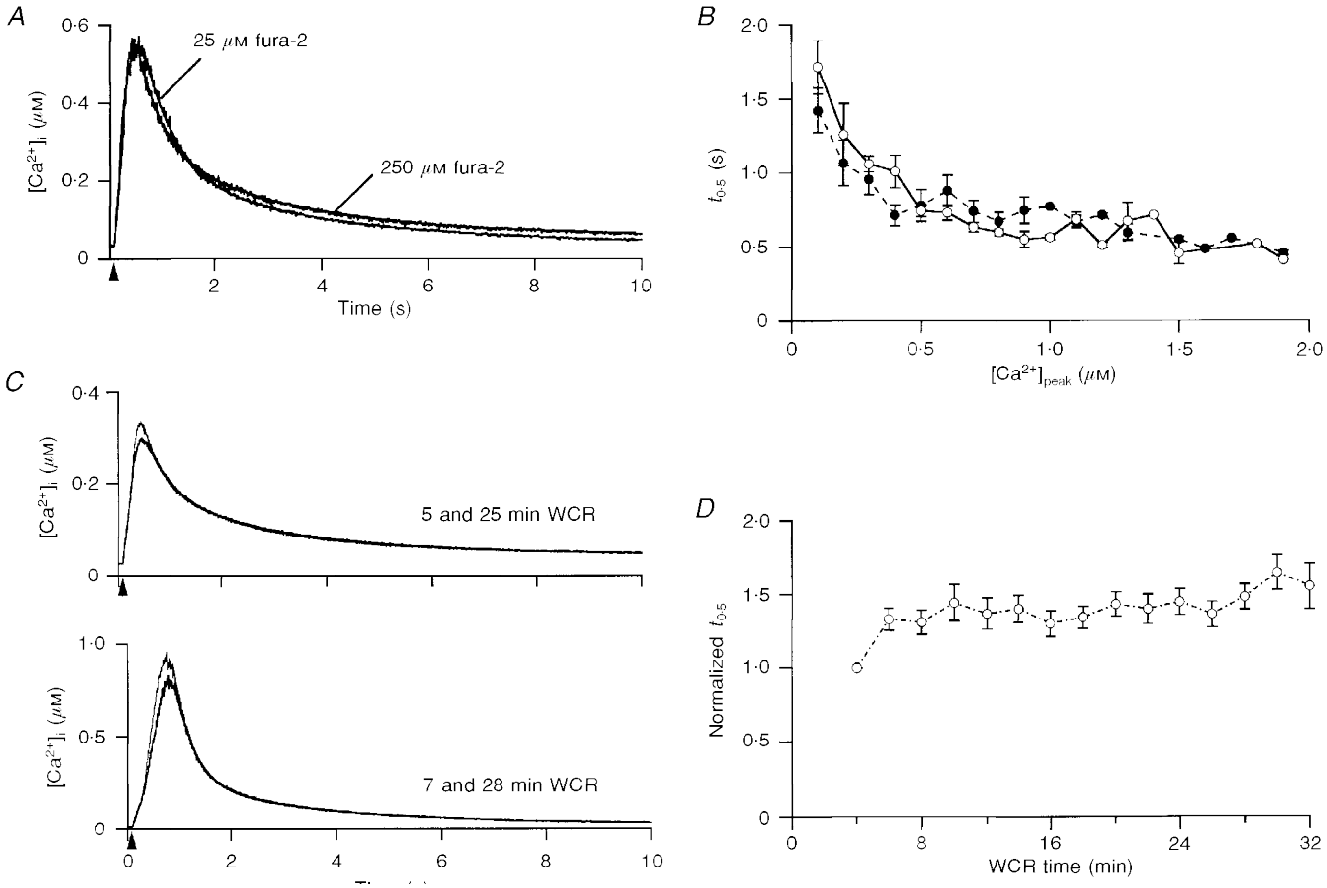

Figure 2. Stability of Ca_i^{2+} transients in WCR

A, Ca_i^{2+} transients elicited in 2 Purkinje cells by 100 ms depolarizations. The cells were dialysed with 25 and 250 μM fura-2, as indicated on the graph. *B*, pooled data for the mean $t_{0.5}$ for Ca_i^{2+} transients, elicited by depolarizations ranging in duration from 20 to 300 ms, in cells dialysed with 25 μM fura-2 (●; 11 cells) or 250 μM fura-2 (○; 14 cells). $t_{0.5}$ values in each cell were binned at increments of 100 nM peak $[Ca^{2+}]_i$. *C*, upper panel, 2 Ca_i^{2+} transients with peak levels in the 300 nM range were elicited by 175 ms depolarizations at the indicated WCR times. Lower panel, similar experiment with a different cell using 250 ms depolarizations, which elicit Ca_i^{2+} transients with peak values close to 1 μM. *D*, pooled data for the mean $t_{0.5}$ as a function of time in WCR (10 cells). For each cell, the $t_{0.5}$ values at different WCR times were normalized to the $t_{0.5}$ at 4 min in WCR. Normalized data were binned in 2 min increments. In *B* and *D*, symbols display the mean and error bars the S.D.

the following, we describe pharmacological and ion-substitution experiments designed to determine the relative contribution of several putative clearance systems to the removal of Ca_i^{2+} from Purkinje cell somata following depolarization-evoked $[Ca^{2+}]_i$ rises.

SERCA pumps

SERCA pumps are one of the well-studied ATP-dependent Ca^{2+} mechanisms in several cells and their presence in cerebellar Purkinje cells has been ascertained by immunocytochemistry (Takei *et al.* 1992, and references therein). To study their contribution to the decay phase of Ca_i^{2+} transients, we used cyclopiazonic acid (CPA) and thapsigargin, specific inhibitors of this ATPase (Inesi & Sagara, 1994). Figure 3 illustrates characteristic examples of the results obtained with 50 μM CPA for Ca_i^{2+} transients peaking in the 100 nM range (Fig. 3*A*) and in the 1–2 μM range (Fig. 3*B*). In both cases, CPA slows significantly the return of $[Ca^{2+}]_i$ to resting levels. Similar results were obtained in seven out of eight cells tested. The effect of CPA was dose dependent, 4 μM ($n = 5$; data not shown) exerting a smaller effect than 50 μM. Thapsigargin had similar actions to CPA when used at 10 μM (4 out of 5 cells; example in Fig. 3*C*). Neither inhibitor affected the resting value of $[Ca^{2+}]_i$.

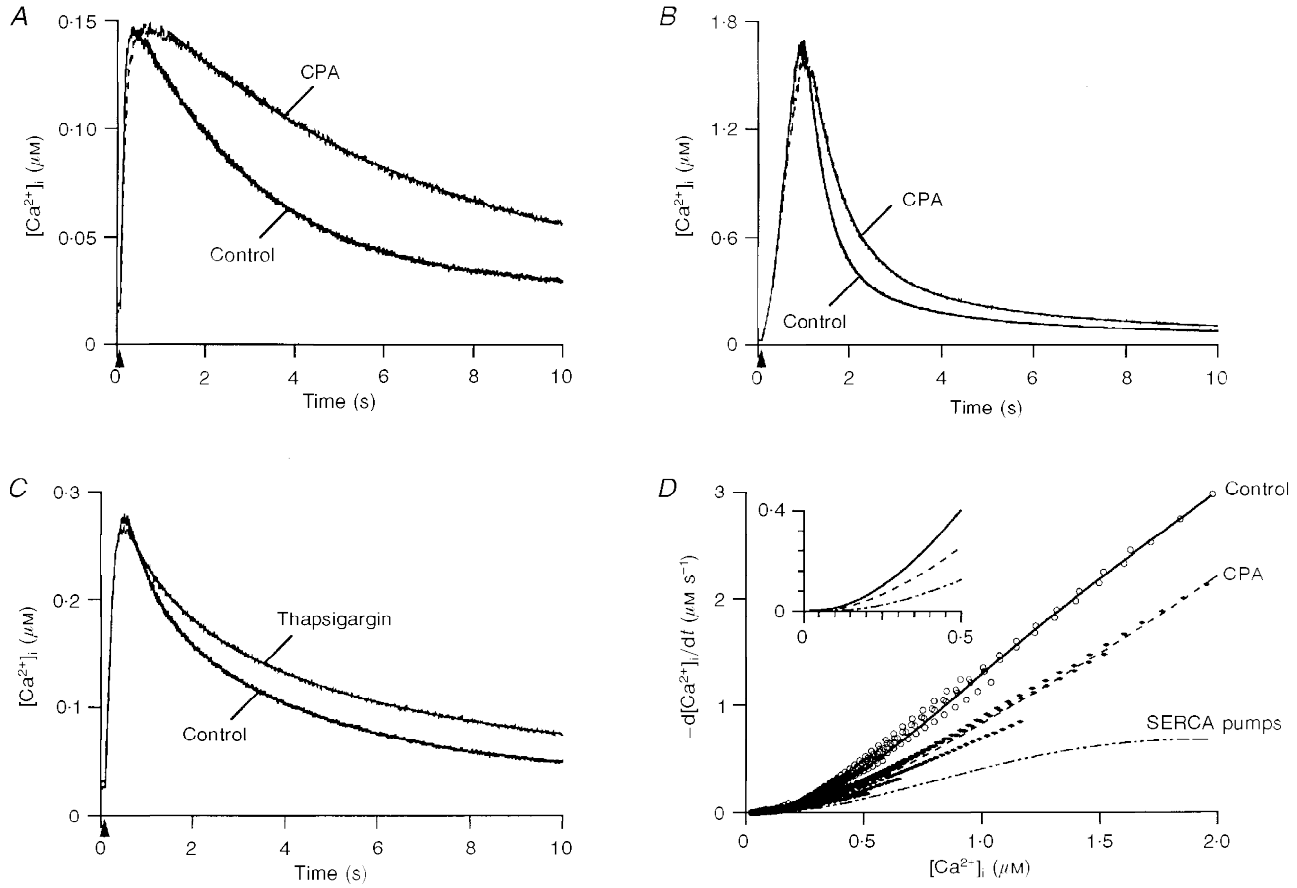

Figure 3. Contribution of SERCA pumps to Ca_i^{2+} clearance

A, effect of cyclopiazonic acid (CPA) on small Ca_i^{2+} transients: superimposed Ca_i^{2+} transients recorded in control external saline and in the presence of 50 μM CPA. The control trace was elicited by a 60 ms depolarization at 9 min in WCR and the CPA trace by a 50 ms depolarization at 21 min WCR. The corresponding $t_{0.5}$ values were 2·2 and 5·2 s, respectively. Superimposed on both traces are the fits of the decay phase by a single exponential, with $t = 2{\cdot}88$ s in control and 6·63 s in CPA. *B*, effect of 50 μM CPA on large Ca_i^{2+} transients: the control trace corresponds to a 220 ms depolarization at 13 min in WCR while the CPA trace was elicited by a 200 ms depolarization at 28 min in WCR. The $t_{0.5}$ values were 0·5 and 0·8 s, respectively. The fit of the decay by a double exponential is superimposed on each trace; τ_1 and τ_2 were 0·52 and 3·56 s in control, and 0·76 and 4·34 s in CPA. *C*, effect of 10 μM thapsigargin on Ca_i^{2+} transients. The control trace was elicited by a 100 ms depolarization at 10·5 min in WCR while the thapsigargin trace results from a 80 ms depolarization at 28 min in WCR. The corresponding $t_{0.5}$ values were 1·6 and 3·6 s, respectively. Fits by a double exponential (superimposed on each trace) yield τ_1 and τ_2 values of 0·69 and 4·07 s in control, and 1·04 and 5·29 s in thapsigargin. *D*, data from 36 Ca_i^{2+} transients (18 in control saline and 18 in CPA) were pooled from 7 cells and analysed in terms of $-d[Ca^{2+}]_i/dt$ as a function of $[Ca^{2+}]_i$. The symbols correspond to the data points and the lines to the fit of the pooled data. The inset illustrates polynomial fits and the resulting subtraction for the low $[Ca^{2+}]_i$ range.

To quantify the contribution of SERCA pumps to Ca_i^{2+} clearance, Ca_i^{2+} transients with similar peak $[Ca^{2+}]_i$ were analysed as detailed in Methods to determine the rate of clearance ($-d[Ca^{2+}]_i/dt$) as a function of $[Ca^{2+}]_i$. Figure 3*D* shows the resulting plots for both conditions (control and CPA; 7 cells). Each plot was fitted with a fifth order polynomial function. The subtraction of the polynomial fit in the presence of CPA from the polynomial fit in control yielded the contribution of SERCA pumps to Ca_i^{2+} clearance. The inset expands the polynomial fits and resulting subtraction for the low $[Ca^{2+}]_i$ range.

Plasma membrane clearance systems

In most cell types it is well known that plasma membrane Ca^{2+} (PMCA) pumps and plasma membrane Na^+–Ca^{2+} exchangers, working in parallel, contribute to the decay of Ca_i^{2+} transients. Several agents (e.g. calmidazolium and La^{3+}) can inhibit PMCA pump activity partially or totally. However, unlike SERCA pump antagonists, they do not have a high specificity for PMCA pumps. Fluorescein analogues such as eosin and carboxyeosin have been demonstrated to be powerful inhibitors of PMCA activity in cardiac myocytes (Bassani, Bassani & Bers, 1995) and in squid giant axon (R. DiPolo & L. Beaugé, personal communication). Thus, we tested the effects of 5,6-succinimidyl carboxyeosin (CE) at 40 μM, a concentration at which this fluorescein analogue can affect SERCA as well as PMCA pumps, but does not interfere with the Na^+–Ca^{2+} exchanger (Bassani *et al.* 1995; R. DiPolo & L. Beaugé, personal communication). To assay the role of PMCA pumps in isolation from SERCA pumps, these experiments were performed in the presence of 50 μM CPA (applied by bath perfusion 8 min prior to the experiment). Figure 4 illustrates the results obtained in the low (Fig. 4*A*) and high range of $[Ca^{2+}]_i$ (Fig. 4*B*). The effect of CE on the time course of decay of Ca_i^{2+} transients was dose dependent, 20 μM ($n = 3$; data not shown) exerting a smaller effect than 40 μM of the inhibitor. There were no significant changes in resting $[Ca^{2+}]_i$, nor on the peak $[Ca^{2+}]_i$ reached by a given depolarization.

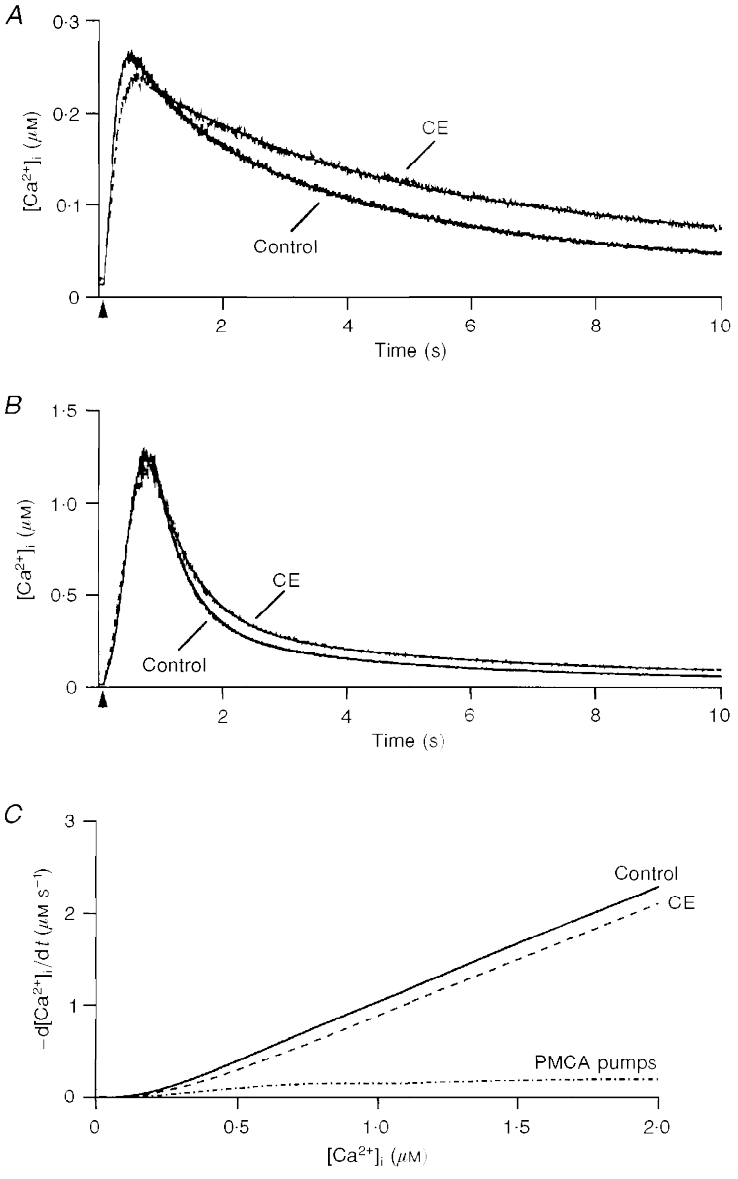

Figure 4. Contribution of PMCA pumps to Ca_i^{2+} clearance

A, effect of 5,6-succinimidyl carboxyeosin (CE) on small Ca_i^{2+} transients: superimposed Ca_i^{2+} transients recorded in control external saline and in the presence of 40 μM CE. The control trace was elicited by a 160 ms depolarization at 13 min in WCR and the CE trace results from a 150 ms depolarization at 25 min in WCR. The corresponding $t_{0.5}$ values were 2·2 and 3·6 s. Superimposed on each trace are the fits of the decay by a double exponential, with τ_1 and τ_2 of 0·78 and 4·06 s in control, and 2·68 and 8·4 s in CE. *B*, effect of 40 μM CE on large Ca_i^{2+} transients: the control trace corresponds to a 210 ms depolarization at 11·5 min in WCR while the CE trace was elicited by a 200 ms depolarization at 25 min in WCR. The $t_{0.5}$ values were 0·55 and 0·66 s, respectively. Time constants of decay (fits are superimposed on each trace) were 0·63 and 4·31 s in control, and 0·53 and 3·57 s in CE. *C*, data from 48 Ca_i^{2+} transients (24 in control saline and 24 in CE) were pooled from 13 cells and analysed in terms of $-d[Ca^{2+}]_i/dt$ as a function of $[Ca^{2+}]_i$.

A similar data analysis to that performed in the experiments with CPA was used to assess the role of PCMA pumps in Ca_i^{2+} clearance. The results are summarized in Fig. 4*C*, which displays the polynomial fits of $-d[Ca^{2+}]_i/dt$ as a function of $[Ca^{2+}]_i$ for transients obtained before and after addition of CE (13 cells), as well as the result of their subtraction, corresponding to the contribution of PMCA pumps to Ca_i^{2+} clearance.

As in the case of PMCA pumps, specific antagonists of the Na^+–Ca^{2+} exchanger are not available. However, monovalent cations such as Li^+, choline and *N*-methyl-D-glucamine (NMDG) cannot substitute for Na^+ in the exchange reaction (Philipson & Nicoll, 1992, and references therein). Therefore, to evaluate the contribution of the Na^+–Ca^{2+} exchanger to Ca_i^{2+} clearance, 125 mM NaCl in the extracellular saline was replaced by equimolar LiCl (leaving 27 mM Na^+ in what will be called hereafter Li^+ saline). In our experimental conditions this lowering of extracellular Na^+ is sufficient to invert the electromotive force for the forward reaction of the exchanger, even at 2 μM Ca_i^{2+}. As illustrated in Fig. 5*A*, the decay of Ca_i^{2+} transients was slowed by Li^+ saline, a result observed in all cells tested

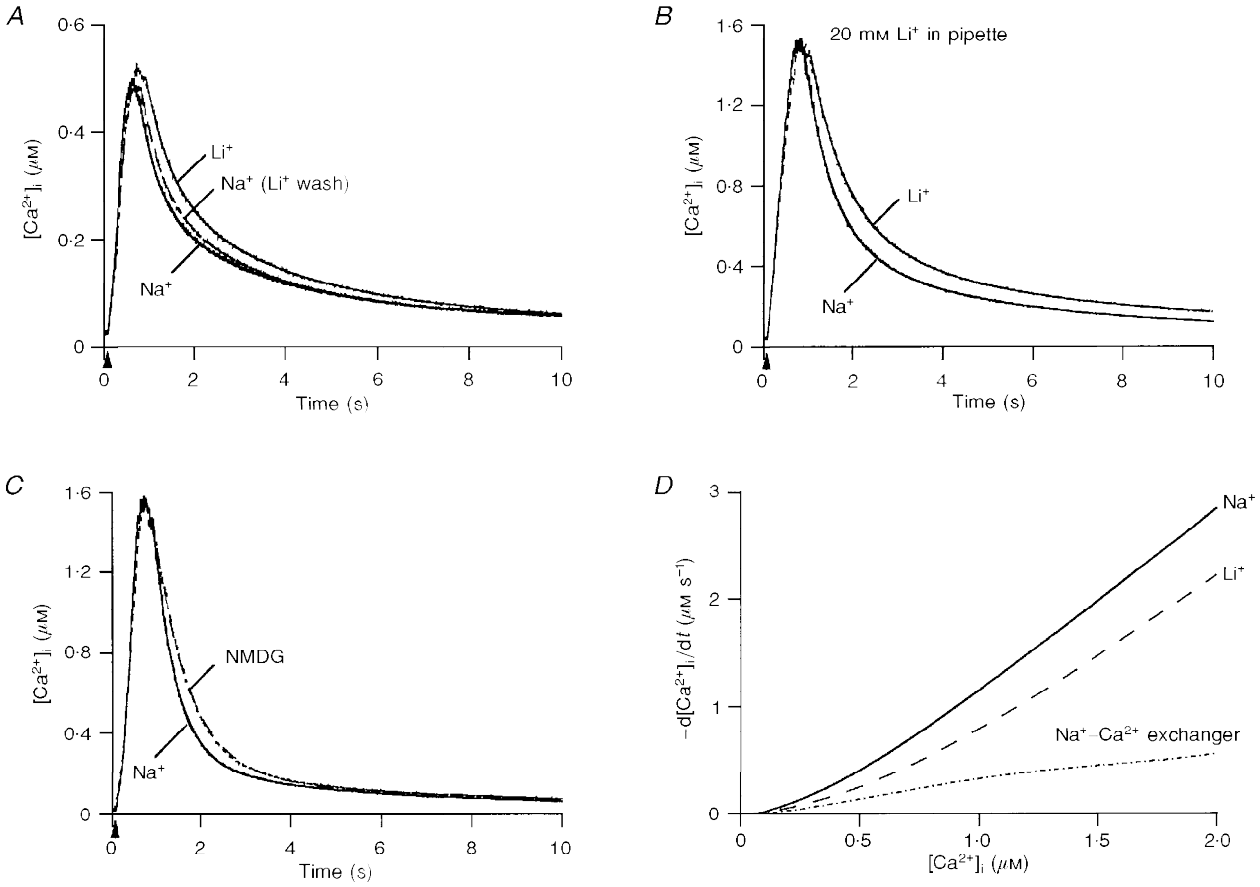

Figure 5. Contribution of the Na^+–Ca^{2+} exchanger to Ca_i^{2+} clearance

A, 3 superimposed Ca^{2+} transients recorded from the same cell in control external saline (Na^+), after changing the bath to a Li^+ saline (Li^+) and upon reintroduction of control saline (Na^+ (Li^+ wash)). The pulse duration and WCR times were: 250 ms and 7 min, respectively, for the Na^+ trace; 275 ms and 12 min, respectively, for the Li^+ trace; and 250 ms and 17 min, respectively, for the Na^+ (Li^+ wash) trace. The corresponding $t_{0.5}$ values were 0·82, 1·05 and 0·89 s, respectively. The fits of the decay by a double exponential are superimposed on each trace; τ_1 and τ_2 were 0·49 and 3·10 s in control, 0·60 and 3·37 s in Li^+, and 0·48 and 2·75 s upon return to Na^+. *B*, 2 superimposed Ca_i^{2+} transients recorded before (Na^+ trace) and after replacement of external Na^+ by Li^+ (Li^+ trace) from a cell in which 20 mM Li^+ was included in the patch pipette. Both transients were elicited by a 150 ms depolarization. WCR times, 9·3 min (Na^+ trace) and 15 min (Li^+ trace); $t_{0.5}$ values, 0·67 and 1·0 s. Double exponential fits of the decay give τ_1 and τ_2 values of 0·61 and 3·42 s in control, and 0·8 and 4·16 s in Li^+. *C*, effect of external Na^+ replacement by NMDG: Ca_i^{2+} transients elicited by 180 ms depolarizations in control external saline (Na^+ trace; 7 min in WCR) and in NMDG saline (NMDG trace; 12·5 min in WCR). The corresponding $t_{0.5}$ values were 0·54 and 0·71 s. Time constants of decay were 0·48 and 3·76 s in control, and 0·70 and 3·86 s in NMDG. *D*, 36 Ca^{2+} transients from 15 cells, 18 for each condition (control and external Li^+) were analysed to calculate $-d[Ca^{2+}]_i/dt$ as a function of $[Ca^{2+}]_i$.

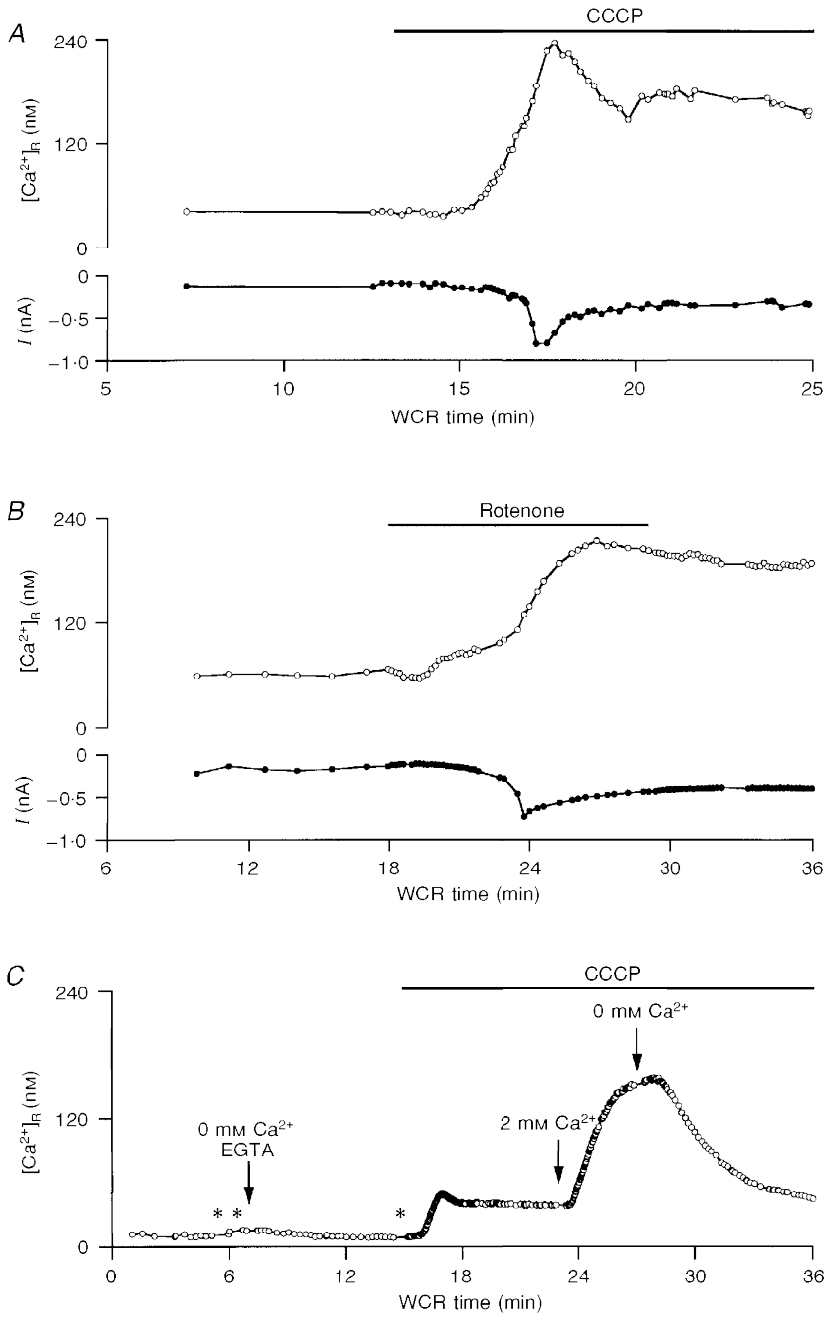

Figure 6. Effects of mitochondrial Ca^{2+} uptake uncouplers on Purkinje cells

A, plot of the resting calcium concentration, $[Ca^{2+}]_R$, (upper panel) and of the holding current at a potential of −60 mV (lower panel) as a function of WCR time. CCCP (2 μM), added to the bath solution during the time indicated by the bar, provoked an increase in $[Ca^{2+}]_R$ and the development of an inward current. *B*, similar experiment, from a different cell, exposed to 10 μM rotenone and 4 μg ml^{-1} oligomycin, which also led to an increase in $[Ca^{2+}]_R$ and the activation of an inward current. *C*, CCCP (2 μM) induced an increase in $[Ca^{2+}]_R$ when the slice was bathed in a Ca^{2+}-free solution, suggesting the presence of a CCCP-sensitive intracellular Ca^{2+} store in Purkinje cell somata. When extracellular Ca^{2+} was reintroduced to the bath solution while CCCP was present, there was an additional increase in $[Ca^{2+}]_R$. Points in time when depolarizations were applied are indicated by ∗; the last depolarization did not elicit any Ca_i^{2+} transient, confirming that external Ca^{2+} was effectively removed (see Methods). The transients elicited by depolarizing pulses are not included in the graph, which plots only the values of $[Ca^{2+}]_R$, as in *A* and *B*.

($n = 15$). In 70% of the cells, the rate of decay upon reintroduction of Na^+ returned to 50–70% of the initial value in control saline ($n = 13$).

External perfusion with Li^+ may lead to the entry of this ion into the cytoplasm, where it could modulate Ca_i^{2+} homeostasis in ways unrelated to its action on the Na^+–Ca^{2+} exchanger (for example, by interfering with the InsP_3 cascade). Two sets of control experiments were performed to rule out this possibility. The first involved substitution of 20 mM CsCl in the internal solution by equimolar LiCl; under this condition, replacement of control saline by Li^+ saline still slowed Ca_i^{2+} transients (Fig. 5*B*). Similar results were obtained in all cells studied ($n = 5$), indicating that the effect of Li^+ on Ca_i^{2+} transients is due to the lowering of the external Na^+ concentration. The second control involved the use of NMDG, an inert cation, as a replacement for Na^+. In seven out of nine cells tested, such replacement slowed the decay of Ca_i^{2+} transients, as displayed in Fig. 5*C*. The effect in these seven cells was smaller than that observed with Li^+ replacement and it was partially reversible in only 33% of the cells ($n = 6$). For a given pulse duration and amplitude, peak $[Ca^{2+}]_i$ values reached in either Li^+ or NMDG were similar to those in control external saline. Replacement of extracellular Na^+ by Li^+ (but not by NMDG) led to small (5–10 nM) increases in the resting level of $[Ca^{2+}]_i$.

Data from the set of experiments in which extracellular Na^+ was replaced by Li^+ (15 cells) were analysed in terms of $-\mathrm{d}[Ca^{2+}]_i/\mathrm{d}t$ as a function of $[Ca^{2+}]_i$. The corresponding polynomial fits, as well as their subtraction, are shown in Fig. 5*D*.

Mitochondria

We next probed the role of mitochondria in Purkinje cell Ca_i^{2+} homeostasis using Ca^{2+} uptake uncouplers. First, we tested the protonophores carbonyl cyanide *p*-(trifluoromethoxy)phenylhydrazone (FCCP) and carbonyl cyanide *m*-chlorophenylhydrazone (CCCP), which dissipate the transmembrane mitochondrial potential and thus release Ca^{2+} from mitochondria preventing further uptake of the ion by the organelle. These protonophores have been widely used to assay the role of mitochondria in Ca_i^{2+} clearance. In our experimental conditions, bath applications of FCCP (4 μM) and CCCP (2 μM) provoked irreversible changes in the membrane conductance and in the resting calcium concentration, $[Ca^{2+}]_R$, of all Purkinje cells tested ($n = 4$ and 5, respectively). Figure 6*A* illustrates a typical example of these changes. Upon addition of the drug, $[Ca^{2+}]_R$ increased gradually from its basal level of 20–40 nM to ~200 nM and remained elevated after washing out the agent. In parallel with this increment in $[Ca^{2+}]_R$, an inward current was generated at the holding potential (−60 mV). Given the ionic conditions, this current is likely to represent activation of Ca^{2+}-dependent Cl^- channels and/or non-specific Ca^{2+}-dependent cationic channels. Addition to the patch pipette of oligomycin (4 μg ml^{-1}) and of 50 mM Hepes did not prevent the changes in $[Ca^{2+}]_R$ or the accompanying inward current ($n = 3$; data not shown).

We also examined the effect of rotenone (10 μM), a specific inhibitor of complex I of the respiratory chain. As shown in Fig. 6*B*, bath applications of this compound mimicked the effects of protonophores both on $[Ca^{2+}]_R$ and on the membrane holding current ($n = 2$). Due to these effects, Ca^{2+} uptake uncouplers were not useful for assaying the role of mitochondria in Ca_i^{2+} clearance in Purkinje cells. It is nonetheless important to determine the source of Ca^{2+} responsible for the increment in $[Ca^{2+}]_R$ caused by agents which disturb mitochondrial metabolism, to compare with results from other preparations (see Discussion). To this effect, two types of experiments were performed. Firstly, voltage-gated Ca^{2+} channels were blocked by bath application of $CdCl_2$ (200 μM) and D600 (methoxyverapamil; 200 μM). This reduced, but did not eliminate, the effects of FCCP or CCCP ($n = 4$; data not shown). Secondly, the effects of protonophores were studied in the absence of external Ca^{2+}. As illustrated in Fig. 6*C*, application of 2 μM CCCP in Ca^{2+}-free saline (no added Ca^{2+} plus 200 μM EGTA) provoked a small but clear increment in $[Ca^{2+}]_R$. Subsequent addition of 2 μM external Ca^{2+} led to a further increase in $[Ca^{2+}]_R$, which reached a steady level close to that attained in cells exposed to CCCP in normal saline. Control experiments showed that, in the absence of protonophores, $[Ca^{2+}]_R$ does not change when external Ca^{2+} is removed. However, in two out of three cells, addition of external Ca^{2+} following a 6–10 min exposure to Ca^{2+}-free saline, led to a rise in $[Ca^{2+}]_R$ similar to that observed upon Ca^{2+} re-admission in the presence of CCCP (data not shown). Taken together these results strongly suggest that mitochondrial uncouplers release Ca^{2+} from mitochondria. However, contribution of Ca^{2+} influx and/or release from other intracellular stores to the observed increase in resting $[Ca^{2+}]_i$ cannot be ruled out (see Discussion).

DISCUSSION

General properties of Ca_i^{2+} decay in cerebellar Purkinje cell somata

This work is the first attempt to characterize the mechanisms governing Ca_i^{2+} clearance in rat cerebellar Purkinje cells. We focused the study on neuronal somata to manipulate accurately the amplitude and duration of local voltage signals leading to $[Ca^{2+}]_i$ rises. It has been shown previously that the somata of Purkinje cells are accurately voltage clamped using tight-seal whole-cell recording techniques, and that the regenerative current responses which may occur in the dendritic compartment following depolarizing pulses do not contribute to the somatic $[Ca^{2+}]_i$ changes (Llano *et al.* 1994). Consequently, our experimental conditions allowed us to explore a wide range of $[Ca^{2+}]_i$ in a reproducible fashion.

It is important to emphasize that we studied the time course of decay of spatially averaged Ca_i^{2+} transients. Confocal

Table 1. Relative contribution of cellular clearance systems to Ca_i^{2+} removal

	0·5 μM Ca_i^{2+}	1 μM Ca_i^{2+}	1·5 μM Ca_i^{2+}	2 μM Ca_i^{2+}
A. Determined contribution (%)				
SERCA pumps	27	31·5	28·5	21
PMCA pumps	21	11·5	8	6
Na^+–Ca^{2+} exchanger	30	25	20	18
Total characterized	78	68	56·5	45
B. Predicted maximal rate of activity (%)				
SERCA 2b pumps	77	93	97	98
SERCA 2a pumps	61	86	93	96
PMCA pumps	95	99	99	99
Na^+–Ca^{2+} exchanger				
High affinity	50	67	75	80
Low affinity	1	2	4	5
Mitochondrial uptake	3	6	9	11

A, the relative percentage contribution of each system to Ca_i^{2+} clearance was calculated for different levels of Ca_i^{2+}, from the polynomial fits to the experimental data summarized in Fig. 7. B, for each system and range of $[Ca^{2+}]_i$, the numbers correspond to the fraction of the maximal rate of activity, calculated as: $([Ca^{2+}]^n/(K_{0.5}{}^n + [Ca^{2+}]^n)) \times 100$, where $K_{0.5}$ and n represent the affinity constant for Ca^{2+} and the number of Ca^{2+} ions transported per cycle per molecule, respectively (Lytton, Westlin, Burk, Shull & MacLennan, 1992). Values for $K_{0.5}$ and n were: SERCA 2b pumps: 0·27 μM, $n = 2$; and SERCA 2a pumps: 0·4 μM, $n = 2$ (Lytton *et al.* 1992); PMCA pumps: 0·11 μM, $n = 2$ (Gill *et al.* 1984); Na^+–Ca^{2+} exchanger, low affinity: 40 μM, $n = 1$; and Na^+–Ca^{2+} exchanger, high affinity: 0·5 μM, $n = 1$ (Gill *et al.* 1984); mitochondria: 16 μM, $n = 1$ (Gunter & Gunter, 1994).

microscopy of Purkinje cells indicates that substantial spatial gradients are achieved when $[Ca^{2+}]_i$ rises in the neuronal somata following climbing fibre stimulation or depolarization in voltage-clamped neurones (Eilers *et al.* 1995). The decay of the spatially averaged Ca_i^{2+} transients measured in the present study (τ_1, ~0·6 s; τ_2, ~3 s) is slower than that observed by Eilers *et al.* (1995) in the subplasmalemmal region of Purkinje cell somata (τ_1, ~0·1 s; τ_2, ~0·8 s). In our work, we observed a double exponential Ca_i^{2+} decay throughout the range of $[Ca^{2+}]_i$ explored (50 nM to 2 μM), reflecting the combined action of endogenous and exogenous calcium buffers as well as cellular calcium clearance systems. Concerning endogenous buffers, calcium-binding proteins such as calbindin and parvalbumin are likely to play key roles in Purkinje cells. Two recent reports support the involvement of calbindin. Firstly, we have found that the buffering capacity of Purkinje cells increases during development, paralleling the increased expression of calbindin D_{28k} (Fierro & Llano, 1996, and references within). Secondly, it has been shown that the amplitude of Ca_i^{2+} transients is significantly larger in Purkinje cells from mice lacking calbindin D_{28k} than in cells from control animals (Airaksinen, Eilers, Garaschuk, Thoenen, Konnerth & Meyer, 1997). This result is in agreement with the fast on-rate and high affinity of calbindin for Ca^{2+}, which would constrain the maximum $[Ca^{2+}]_i$ rise attained for a given influx and set an upper limit to the speed of its decay (Sala & Hernandez-Cruz, 1990; Lledo, Somasundaram, Morton, Emson & Mason, 1992; Chard, Bleakman, Christakos, Fullmer & Miller, 1993). There are no physiological data pertaining to the involvement of parvalbumin in Purkinje cells. In other systems, this protein also limits $[Ca^{2+}]_i$ rises and slows their decay (Chard *et al.* 1993). In the present work, we find the values of the two decay time constants to be independent of peak $[Ca^{2+}]_i$, whereas the contribution of the faster time constant increases with $[Ca^{2+}]_i$. Such behaviour could result from the progressive acceleration, as a function of $[Ca^{2+}]_i$, of clearance mechanisms, particularly those with fast kinetics and low Ca^{2+} affinity.

Relative contribution of the mechanisms which participate in Ca_i^{2+} clearance in Purkinje cell somata

We have compared Ca_i^{2+} transients with similar peak values in control and experimental conditions in order to calculate the rates of clearance. Although similar Ca_i^{2+} peak responses do not necessarily imply similar Ca_i^{2+} loads, this assumption is strongly supported by the stability during long whole-cell recording periods of both the peak $[Ca^{2+}]_i$ induced by a given stimulus and the time course of decay of the transients. Both parameters indicate that Ca^{2+} influx and/or release and the endogenous Ca^{2+}-binding ratio remain constant during the experiments.

Figure 7 summarizes the Ca_i^{2+} clearance rates as a function of $[Ca^{2+}]_i$ for the three systems investigated in the present work: SERCA pumps, PMCA pumps and the Na^+–Ca^{2+} exchanger. Since the curves were obtained by subtraction (see Methods), no correction is needed for Ca^{2+} diffusion to the pipette. The relative contribution of each system, calculated from these curves for four values of $[Ca^{2+}]_i$, is given in Table 1A. At the lowest range of $[Ca^{2+}]_i$, the combined action of the three systems can account for a high fraction (78%) of the removal process. As $[Ca^{2+}]_i$ increases, their total contribution declines, reaching 45% at 2 μM Ca_i^{2+}. The relative contribution of the clearance systems varies as a function of $[Ca^{2+}]_i$. In the low range, the proportion of Ca_i^{2+} removed by SERCA pumps, PMCA pumps and the Na^+–Ca^{2+} exchanger is balanced. At 2 μM the major contributors are the SERCA pumps (21%) and the Na^+–Ca^{2+} exchanger (18%), whereas PMCA pumps account for only 6% of Ca_i^{2+} clearance. Table 1B presents the fraction of the maximal rate of activity expected from each of these systems, as well as for mitochondria, when allowance is made for their Ca^{2+} affinity and for the number of Ca^{2+} ions transported per molecule (see Table 1 legend). These calculations indicate that SERCA pumps will be close to saturation at Ca_i^{2+} levels above 1·5 μM, whereas PMCA pumps will already be near saturation at 0·5 μM. The predictions are in accordance with the data displayed in Fig. 7, which shows that while clearance rates for PMCA

pumps level slightly above 0·5 μM Ca_i^{2+}, rates for SERCA pumps continue to increase up to 1·5 μM Ca_i^{2+}.

The involvement of SERCA pumps in Purkinje cell Ca_i^{2+} homeostasis is in accordance with immunocytochemical studies demonstrating high levels of SERCA pumps of the 2b subtype ($K_{0.5}$, ~0·27 μM) and lower levels for the 2a subtype ($K_{0.5}$, ~0·4 μM) (Takei *et al.* 1992, and references therein). PMCA pumps have also been described in Purkinje cells. The PMCA pump type 2 is the most abundant, having a 10-fold higher concentration than other pumps of the same family (Tolosa de Talamoni *et al.* 1993). Additionally, it is considered that PMCA pump types 1 and 4 are present in almost all cell types and participate in regulating resting $[Ca^{2+}]_i$. Although eosin derivatives have not been studied before in Purkinje cells, the contribution we calculate for PMCA pumps is similar to that obtained in other cell types with different PMCA pump blockers (Herrington, Park, Babcok & Hille, 1996) and to the one expected for a system with high affinity, low capacity and slow transport turnover.

It is worth noting that agents which interfered with SERCA or PMCA pumps, as well as ionic substitutions affecting the Na^+–Ca^{2+} exchanger, did not alter resting Ca_i^{2+} levels. In this context, one must consider that the resting $[Ca^{2+}]_i$ in Purkinje cells is quite low and that it is not affected by removal of external Ca^{2+}, indicating that the passive leak of Ca^{2+} into the cell somata is small. The clearance systems are therefore expected to work at slow rates under basal conditions. Since in our experiments only one putative clearance system was blocked at a given time, any small $[Ca^{2+}]_i$ increase would be compensated for by the activation of the other systems.

The Na^+–Ca^{2+} exchanger

The Na^+–Ca^{2+} exchanger has been shown to participate in the regulation of Ca_i^{2+} homeostasis and of exocytosis in neuronal cells (e.g. Reuter & Porzig, 1995). Our analysis shows a small but sustained increase in the clearance performed by this system as $[Ca^{2+}]_i$ increases, a similar result to that reported for chromaffin cells (Herrington *et al.* 1996). These findings can be explained by a system with two sites for Ca_i^{2+} transport, one with high affinity and the other with low affinity, as proposed from studies of the Na^+–Ca^{2+} exchanger in synaptosomes (Gill, Chueh & Whitlow, 1984). Alternatively, a single site whose affinity for Ca^{2+} decreases with increments in $[Ca^{2+}]_i$ can account for the results. In either case, no saturation is expected for the Na^+–Ca^{2+} exchanger in the $[Ca^{2+}]_i$ range covered by our experiments. The presence of the Na^+–Ca^{2+} exchanger has not been documented immunocytochemically in Purkinje cells at the single cell level. However, antibodies against mRNA encoding the cardiac type of the exchanger, isolated from cerebellar granular cells, label the Purkinje cell layer (Marlier, Jian Tang & Grayson, 1993). The modest contribution of the exchanger to Purkinje cell Ca_i^{2+} clearance observed in the present work indicates that while the exchanger is present in Purkinje cells, its density is much lower than in other tissues such as cardiac muscle where this system plays a predominant role in governing Ca_i^{2+} homeostasis (reviewed by Philipson & Nicoll, 1992).

Mitochondria

Protonophores, as well as the respiratory chain inhibitor rotenone, led to significant increases in the basal levels of Ca_i^{2+} in Purkinje cells. Exposure to agents which interfere with mitochondrial Ca^{2+} uptake induce changes in resting

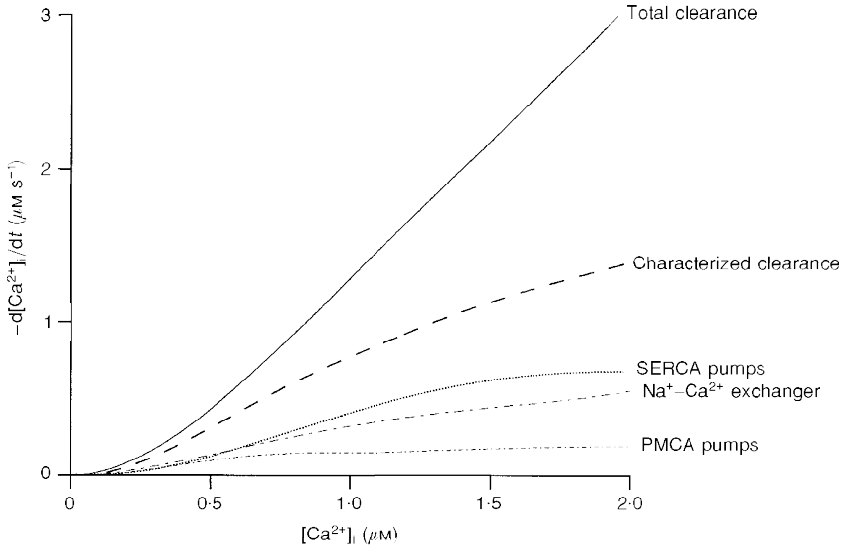

Figure 7. Summary of Ca_i^{2+} clearance in rat cerebellar Purkinje cell somata

Total Ca^{2+} clearance rate is presented in comparison with the rate of the different components characterized during the present study. Clearance rate is plotted as a function of the $[Ca^{2+}]_i$ in the range between 50 nM and 2 μM.

$[Ca^{2+}]_i$ that vary considerably amongst cell types. Thus, protonophores do not affect resting $[Ca^{2+}]_i$ in chromaffin cells (Herrington *et al.* 1996) or in cortical pyramidal neurones (Markram, Helm & Sackmann, 1995). On the other hand, protonophores and/or respiratory chain inhibitors provoke augmentations in $[Ca^{2+}]_i$ in mammalian neurones dissociated from the nucleus basalis (Tatsumi & Katayama, 1993), from the cerebellum (Kaplin, Snyder & Linden, 1996) and from the hippocampus (Villalba *et al.* 1994; Nowicky & Duchen, 1998), as well as in bullfrog sympathetic neurones (Friel & Tsien, 1994). Some of the reported alterations in Ca_i^{2+} homeostasis are likely to involve ATP depletion and subsequent Ca_i^{2+} release from intracellular stores. In fact, Kaplin *et al.* (1996) identify InsP_3R-sensitive stores as the target for the large $[Ca^{2+}]_i$ rises induced by cyanide in PC12 cells and in dissociated cerebellar Purkinje cells. However, in some of the studies cited above as well as in the present work, the $[Ca^{2+}]_i$ elevations do not appear to be secondary to changes in intracellular pH or to ATP depletion, since they are obtained in cells dialysed with millimolar concentrations of ATP and with high pH buffering power (Tatsumi & Katayama, 1993; the present study). Furthermore, oligomycin, when used in conjunction with protonophores to prevent ATP hydrolysis, does not impede the $[Ca^{2+}]_i$ rises (Villalba *et al.* 1994; the present study). The source of Ca^{2+} ions responsible for these $[Ca^{2+}]_i$ elevations appears to be dual. On the one hand, Ca^{2+} channel blockers reduce the increase in $[Ca^{2+}]_i$, suggesting that the plasma membrane permeability to Ca^{2+} is altered by mitochondrial uncouplers and inhibition of the respiratory chain (Nowicky & Duchen, 1998; the present study). On the other hand, the $[Ca^{2+}]_i$ rises can be obtained in the absence of extracellular Ca^{2+}, indicating release from intracellular stores (Villalba *et al.* 1994; the present study). Regardless of the source of Ca^{2+}, the possibility must be envisaged that some of the effects of mitochondrial uncouplers are due to release of neurotansmitters from other neurones in the preparation, and subsequent activation of receptors coupled to intracellular Ca^{2+} release pathways (e.g. metabotropic glutamate receptors).

During the present study, the effects of protonophores and rotenone on Purkinje cell membrane conductance and resting $[Ca^{2+}]_i$ hindered further characterization of the role of mitochondria in Ca_i^{2+} removal following depolarization-evoked $[Ca^{2+}]_i$ rises. In other preparations, namely bullfrog sympathetic neurones (Friel & Tsien, 1994), rat dorsal root ganglion neurones (Thayer & Miller, 1990) and chromaffin cells (Herrington *et al.* 1996), a dominant role of mitochondria in Ca_i^{2+} clearance has been postulated. In neurones from the rat nucleus basalis (Tatsumi & Katayama, 1993) and in rat isolated neurohypophysial nerve endings (Stuenkel, 1994) both mitochondria and Ca^{2+} pumps have been found to play an important role in Ca_i^{2+} clearance. Finally, in rat septal neurones (Bleakman, Roback, Wainer, Miller & Harrison, 1993) and in cortical pyramidal neurones (Markram *et al.* 1995) mitochondria do not contribute to Ca_i^{2+} clearance whereas SERCA pumps play a crucial role. This variability between different cell types in mitochondrial contribution to Ca_i^{2+} clearance might result from differences in the regulation of mitochondrial Ca^{2+} transport (Gunter & Gunter, 1994).

Limitations of the present study

Our results are likely to correspond to a lower limit for the contribution of the various systems studied, for two reasons. Firstly, the turnover of Ca^{2+} pumps as well as of the Na^+–Ca^{2+} exchanger is highly temperature dependent (Q_{10}, 2–4) and our experiments were done at 20–24 °C. Secondly, we have studied each clearance system by interfering with it either through specific inhibitors or by ionic replacement, while leaving other systems unaltered. Under these conditions, unblocked mechanisms should be able to compensate, at least partially, for the inhibition of the blocked system. Furthermore, although we have used inhibitors at doses which induce maximal inhibition in isolated transport systems and allowed for several minutes of incubation, we cannot ensure that such doses are sufficient to inhibit totally the system in question in a brain slice. These factors may partially explain the relatively high percentage of total Ca_i^{2+} clearance which remains unaccounted for by the present study. Furthermore, at least 15% of the Ca_i^{2+} removal could correspond to diffusion of the ion towards the patch pipette (see Fig. 3*D* in Herrington *et al.* 1996). On the other hand, mechanisms not yet identified may contribute to Purkinje cell Ca_i^{2+} clearance. Thus, in cerebellar microsomal fractions it has been observed that cyclopiazonic acid and thapsigargin can inhibit only 50–75% of ATP-dependent Ca^{2+} transport (Michelangeli, DaSilva, Sayers & Brown, 1992). This suggests that some or probably all cerebellar cells possess intracellular compartments with Ca^{2+}-ATPases distinct from SERCA pumps. These pumps could be partially responsible for the component of Ca_i^{2+} clearance unaccounted for in our work. Finally, further experiments need to be carried out in Purkinje cells to determine the role played by mitochondria in the clearance of Ca_i^{2+} following depolarization-induced $[Ca^{2+}]_i$ rises.

Airaksinen, M. S., Eilers, J., Garaschuk, O., Thoenen, H., Konnerth, A. & Meyer, M. (1997). Ataxia and altered dendritic calcium signaling in mice carrying a targeted null mutation of the calbindin D28k gene. *Proceedings of the National Academy of Sciences of the USA* **94**, 1488–1493.

Bassani, R. A., Bassani, J. W. & Bers, D. M. (1995). Relaxation in ferret ventricular myocytes: role of the sarcolemmal Ca ATPase. *Pflügers Archiv* **430**, 573–578.

Bleakman, D., Roback, J. D., Wainer, B. H., Miller, R. J. & Harrison, N. L. (1993). Calcium homeostasis in rat septal neurons in tissue culture. *Brain Research* **600**, 257–267.

Chard, P., Bleakman, D., Christakos, S., Fullmer, C. S. & Miller, R. J. (1993). Calcium buffering properties of calbindin D_{28k} and parvalbumin in rat sensory neurones. *Journal of Physiology* **472**, 341–357.

Denk, W., Sugimori, M. & Llinás, R. (1995). Two types of calcium response limited to single spines in cerebellar Purkinje cells. *Proceedings of the National Academy of Sciences of the USA* **92**, 8279–8282.

Eilers, J., Callewaert, G., Armstrong, C. & Konnerth, A. (1995). Calcium signaling in a narrow somatic submembrane shell during synaptic activity in cerebellar Purkinje neurons. *Proceedings of the National Academy of Sciences of the USA* **92**, 10272–10276.

Fierro, L. & Llano, I. (1996). High endogenous calcium buffering in Purkinje cells from rat cerebellar slices. *Journal of Physiology* **496**, 617–625.

Friel, D. D. & Tsien, R. W. (1994). An FCCP-sensitive store in bullfrog sympathetic neurons and its participation in stimulus-evoked changes in $[Ca^{2+}]_i$. *Journal of Neuroscience* **14**, 4007–4024.

Gill, D. L., Chueh, S.-H. & Whitlow, C. L. (1984). Functional importance of the synaptic plasma membrane calcium pump and sodium-calcium exchanger. *Journal of Biological Chemistry* **259**, 10807–10813.

Gunter, K. K. & Gunter, T. E. (1994). Transport of calcium by mitochondria. *Journal of Bioenergetics and Biomembranes* **26**, 471–485.

Herrington, J., Park, Y. B., Babcock, D. F. & Hille, B. (1996). Dominant role of mitochondria in clearance of large Ca^{2+} loads from rat adrenal chromaffin cells. *Neuron* **16**, 219–228.

Inesi, G. & Sagara, Y. (1994). Specific inhibitors of intracellular Ca^{2+} transport ATPases. *Journal of Membrane Biology* **141**, 1–6.

Kano, M., Schneggenburger, R., Verkhratsky, A. & Konnerth, A. (1995). Depolarization-induced calcium signals in the somata of cerebellar Purkinje neurons. *Neuroscience Research* **24**, 87–95.

Kaplin, A. I., Snyder, S. H. & Linden, D. J. (1996). Reduced nicotinamide adenine dinucleotide-selective stimulation of inositol 1,4,5-trisphosphate receptors mediates hypoxic mobilization of calcium. *Journal of Neuroscience* **15**, 2002–2011.

Khodakhah, K. & Ogden, D. (1995). Fast activation and inactivation of inositol trisphosphate-evoked Ca^{2+} release in rat cerebellar Purkinje neurones. *Journal of Physiology* **487**, 343–358.

Lev-Ram, V., Miyakawa, H., Lasser-Ross, N. & Ross, W. N. (1992). Calcium transients in cerebellar Purkinje neurons evoked by intracellular stimulation. *Journal of Neurophysiology* **68**, 1167–1177.

Llano, I., DiPolo, R. & Marty, A. (1994). Calcium-induced calcium release in cerebellar Purkinje cells. *Neuron* **12**, 663–673.

Lledo, P. M., Somasundaram, B., Morton, A. J., Emson, P. C. & Mason, W. T. (1992). Stable transfection of calbindin D_{28k} into the GH_3 cell line alters calcium currents and intracellular calcium homeostasis. *Neuron* **9**, 943–954.

Lytton, J., Westlin, M., Burk, S. E., Shull, G. E. & MacLennan, D. H. (1992). Functional comparisons between isoforms of the sarcoplasmic or endoplasmic reticulum family of calcium pumps. *Journal of Biological Chemistry* **267**, 14483–14489.

Markram, H., Helm, J. P. & Sakmann, B. (1995). Dendritic calcium transients evoked by single back-propagating action potentials in rat neocortical pyramidal neurons *Journal of Physiology* **485**, 1–20.

Marlier, L. N. J.-L., Jian Tang, T. Z. & Grayson, D. R. (1993). Regional distribution in the rat central nervous system of a mRNA encoding a portion of the cardiac sodium/calcium exchanger isolated from cerebellar granule neurons. *Molecular Brain Research* **20**, 21–39.

Marty, A. & Llano, I. (1995). Modulation of inhibitory synapses in the mammalian brain. *Current Opinion in Neurobiology* **5**, 335–341.

Michelangeli, F., DaSilva, A., Sayers, L. & Brown, G. (1992). The effects of thimerosal and cyclopiazonic acid on the Ca^{2+} pumps from rat cerebellum microsomes. *Biochemical Society Transactions* **20**, 205S.

Miyakawa, H., Lev-Ram, V., Lasser-Ross, N. & Ross, W. N. (1992). Calcium transients evoked by climbing fiber and parallel fiber synaptic inputs in guinea pig cerebellar neurons. *Journal of Neuroscience* **68**, 1178–1189.

Neher, E. (1995). The use of fura-2 for estimating Ca buffers and Ca fluxes. *Neuropharmacology* **34**, 1423–1442.

Nowicky, A. V. & Duchen, M. R. (1998). Changes in $[Ca^{2+}]_i$ and membrane currents during impaired mitochondrial metabolism in dissociated rat hippocampal neurons. *Journal of Physiology* **507**, 131–145.

Ogden, D. (1996). Intracellular calcium release in central neurones. *Seminars in the Neurosciences* **8**, 281–291.

Philipson, K. D. & Nicoll, D. A. (1992). Sodium-calcium exchange. *Current Opinion in Cell Biology* **4**, 678–683.

Plessers, L., Eggermont, J. A., Wuytack, F. & Casteels, R. (1991). A study of the organellar Ca^{2+}-transport ATPase isozymes in pig cerebellar Purkinje neurons. *Journal of Neuroscience* **11**, 650–656.

Regehr, W. G. & Tank, D. W. (1994). Dendritic calcium dynamics. *Current Opinion in Neurobiology* **4**, 373–382.

Reuter, H. & Porzig, H. (1995). Localization and functional significance of the Na^+/Ca^{2+} exchanger in presynaptic boutons of hippocampal cells in culture. *Neuron* **15**, 1077–1084.

Sakurai, M. (1990). Calcium is an intracellular mediator of the climbing fiber in induction of cerebellar long-term depression. *Proceedings of the National Academy of Sciences of the USA* **87**, 3383–3385.

Sala, F. & Hernández-Cruz, A. (1990). Calcium diffusion modeling in a spherical neuron. *Biophysical Journal* **57**, 313–324.

Stuenkel, E. L. (1994). Regulation of intracellular calcium and calcium buffering properties of rat isolated neurohypophysial nerve endings. *Journal of Physiology* **481**, 251–271.

Takei, K., Stukenbrok, H., Metcalf, A., Mignery, G. A., Südhof, T. C., Volpe, P. & De Camilli, P. (1992). Ca^{2+} stores in Purkinje neurons: Endoplasmic reticulum subcompartments demonstrated by the heterogeneous distribution of the $InsP_3$ receptor, Ca^{2+} ATPase and calsequestrin. *Journal of Neuroscience* **12**, 489–505.

Tank, D. W., Sugimori, M., Connor, J. A. & Llinás, R. R. (1988). Spatially resolved calcium dynamics of mammalian Pukinje cells in cerebellar slice. *Science* **242**, 773–777.

Tatsumi, H. & Katayama, Y. (1993). Regulation of the intracellular free calcium concentration in acutely dissociated neurones from rat nucleus basalis. *Journal of Physiology* **464**, 165–181.

Thayer, S. A. & Miller, R. J. (1990). Regulation of the intracellular free calcium concentration in single rat dorsal root ganglion neurones *in vitro*. *Journal of Physiology* **425**, 85–115.

Tolosa de Talamoni, N., Smith, C. A., Wasserman, R. H., Beltramino, C., Fullmer, C. S. & Penniston, J. T. (1993). Immunocytochemical localization of the plasma membrane calcium pump, calbindin-D_{28k} and parvalbumin in Purkinje cells of avian and mammalian cerebellum. *Proceedings of the National Academy of Sciences of the USA* **90**, 11949–11953.

Villalba, M., Martínez-Serrano, A., Gómez-Puertas, P., Blanco, P., Börner, C., Villa, A., Casado, M., Giménez, C., Pereira, R., Bogonez, E., Pozzan, T. & Satrústegui, C. (1994). The role of pyruvate in neuronal calcium homeostasis. *Journal of Biological Chemistry* **269**, 2468–2476.

Acknowledgements

We thank A. Marty for discussions throughout the course of this study, L. Forti for comments on the manuscript and C. Auger and C. Pouzat for aid on analysis routines. This work was supported by the Max-Planck-Gesellschaft and the Hildegard Doerenkamp–Gerhard Zbinden Foundation. R. DiPolo was a visiting fellow under the auspices of the CONICIT (grant S1-97001765) and the Deutscher Akademischer Austausschdienst. L. Fierro was supported by a doctoral fellowship from the Colombian Institute for the Development of Science and Technology (COLCIENCIAS).

Corresponding author

I. Llano: Arbeitsgruppe Zelluläre Neurobiologie, Max-Planck-Institut für Biophysikalische Chemie, Am Fassberg, D37070 Göttingen, Germany.

Email: illano@gwdg.de

Author's present address

L. Fierro: Department of Physiology, University of Oxford, Parks Road, Oxford OX1 3PT, UK.